



ADVANCING MEP SEMANTIC SEGMENTATION WITH DEEP LEARNING AND BIM-DERIVED SYNTHETIC POINT CLOUDS

Hongzhe Yue¹, Qian Wang^{1,*}, Xinyi Feng² and Yangzhi Yan¹

¹ School of Civil Engineering, Southeast University, China

² China Yangtze Power Co., Ltd., China

*Corresponding author. Email: qianwang@seu.edu.cn

Abstract

This paper proposes the Ray-Based Laser Scanning and Intersection Algorithm (RBLISA) to generate synthetic point clouds for Mechanical, Electrical, and Plumbing (MEP) systems using BIM models, addressing the lack of MEP datasets for deep learning-based semantic segmentation. Twenty comparative experiments were conducted to assess the performance across different training datasets, synthetic point cloud generation methods. The results show that RBLISA-generated synthetic point clouds outperform those from uniform sampling by 3.32% in mean Intersection over Union (mIoU). Additionally, increasing the volume of synthetic samples improves overall accuracy (OA) and mIoU, surpassing the performance of models trained with real point clouds.

Introduction

Building Information Modeling (BIM) plays a pivotal role in the management and maintenance of building facilities by offering comprehensive semantic and geometric data. As-built BIM models capture the current state of facilities, aiding in improving maintenance workflows and operational efficiency (Xiong et al., 2013).

Mechanical, Electrical, and Plumbing (MEP) Building Information Modeling (BIM) plays a pivotal role in the management and maintenance of building facilities by offering comprehensive semantic and geometric data. As-built BIM models capture the current state of facilities, aiding in improving maintenance workflows and operational efficiency.

In recent years, three-dimensional (3D) laser scanning, especially terrestrial laser scanning (TLS), has demonstrated high accuracy and efficiency in capturing detailed geometric data, making it an effective method for 3D reconstruction (Wang et al., 2022). A 3D laser scanner emits infrared laser beams and measures the distance to objects based on the reflected signals. By capturing distances from multiple angles, the scanner generates a complete set of point cloud data that accurately represents the 3D geometry of the scanned environment. However, point cloud data, while rich in geometric detail, often lacks semantic information, necessitating further

processing to identify and classify objects within the data. Traditional object recognition methods, such as those based on geometric shape descriptors, hard-coded knowledge, supervised learning, or BIM-vs.-Scan (Wang et al., 2020), rely on predefined human knowledge and extensive parameter tuning. These methods become inadequate when dealing with MEP components that have extensive occlusions and irregular shapes.

Over the past few years, deep learning (DL) algorithms such as PointNet and PointNet++ have shown significant potential in processing point clouds for tasks such as segmentation and completion (Yue et al., 2025; Yue et al., 2024a). DL algorithms significantly reduce reliance on manually designed features by autonomously learning and extracting complex data features from large labeled training datasets, achieving better performance (Yin et al., 2021; Zhang et al., 2022). However, DL often requires large amounts of sample data for training. Compared to images, point cloud data acquisition relies on scanning at multiple stations with a laser scanner, which is extremely time-consuming and labor-intensive. Additionally, labeling point cloud data is also more challenging than labeling image data. Therefore, obtaining a large amount of labeled point cloud data is crucial for DL-based model reconstruction.

BIM-driven synthetic point cloud generation has recently gained traction as a cost-effective solution for producing labeled point clouds, streamlining DL model training (Tang et al., 2022; Tang et al., 2023). Current research predominantly targets synthetic point cloud generation for indoor environments and bridge structures, yielding notable improvements in segmentation accuracy (Lamas et al., 2024; Tang et al., 2023; Won et al., 2020; Zhai et al., 2022; Zhang and Zou, 2023). Nevertheless, limited studies address the generation of synthetic point clouds tailored for MEP systems. The potential of synthetic point clouds to enhance MEP segmentation accuracy remains largely unexplored. Conventional uniform sampling methods used for synthetic point cloud generation may fail to accurately represent real-world occlusions, necessitating the development of specialized approaches for MEP scenarios.

To address this gap, this study proposes a method to generate synthetic point clouds from BIM models

specifically for MEP scenes by simulating the real laser scanning process. To validate the proposed method, this study compares the semantic segmentation performance on MEP scenes with different approaches for generating synthetic point clouds, and different training datasets.

Method

Proposed Method for Generating Synthetic Point Clouds for MEP Scenes

This study introduces a method for generating synthetic point clouds for MEP scenes using BIM models. The overall workflow is illustrated in Figure 1. Initially, the BIM model is converted into the OBJ format, which is then processed using the Trimesh library in Python. Following this, synthetic point clouds are generated using the Ray-based Laser Scanning and Intersection Algorithm (RBLISA). The detailed steps of the RBLISA include three steps: Simulating Laser Scanner Positions, Setting Scanning Parameters and Error Simulation, and Intersection with Triangle Mesh.

Simulating Laser Scanner Positions: The RBLISA begins by simulating the positions of the laser scanner based on human-accessible areas. The scanner positions are chosen to avoid areas occupied by equipment such as pumps and tanks, while ensuring sufficient spacing between each scanning position.

Setting Scanning Parameters and Error Simulation: Next, the scanning parameters, such as vertical and horizontal resolution, are determined based on the actual specifications of the laser scanner. To simulate real-world conditions, measurement errors are also introduced. Synthetic laser rays are then generated accordingly.

Intersection with Triangle Mesh: The core of the RBLISA is the Ray Intersections with Triangle Mesh (RITM) algorithm. This algorithm checks for intersections between each laser ray and the scene's triangle mesh. The

closest intersection points are recorded and used to generate the synthetic point clouds. These points include relevant data such as material, color, and category. The pseudo-code for the RITM this method is shown in Algorithm 1.

Algorithm 1: Ray Intersections with Triangle Mesh algorithm

- intersection_points ← []
- For each direction ∈ D:
 - $d_{min} ← ∞$
 - For each mesh_part ∈ scene.geometry:
 - $h ← \text{mesh_part.ray.intersects_location}(direction)$
 - If h :
 - $d ← \|h - P_s\|$
 - If $d < d_{min}$:
 - $d_{min} ← d$
 - closest_intersection ← (h, material, color, category)
 - If closest_intersection:
 - intersection_points.append(closest_intersection)
- return intersection_points

Figure 2 shows an example of the synthetic point cloud generation process using the RBLISA method. Firstly, the virtual laser scanner position is determined, as indicated by the green mark in Figure 2 (a). Then, the simulated laser rays are generated and the intersections between laser rays and the model's triangular triangle mesh are calculated, as shown in Figure 2 (b). Eventually, the synthetic point clouds of the MEP scene are generated, and the 3D view and plane view are shown in Figure 2 (c) and Figure 2 (d), respectively.

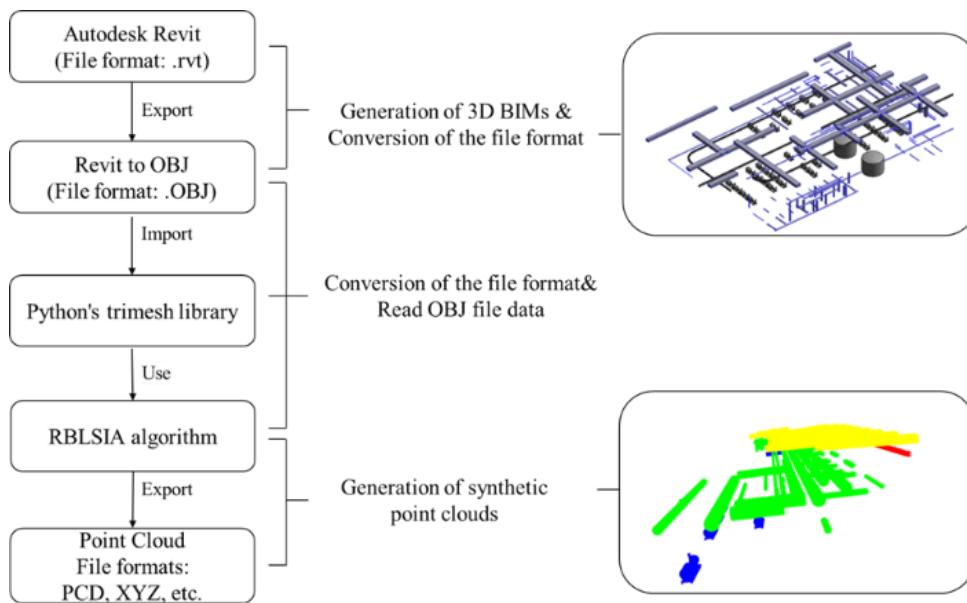


Figure 1: Process of generating synthetic point clouds for MEP scene from BIM.

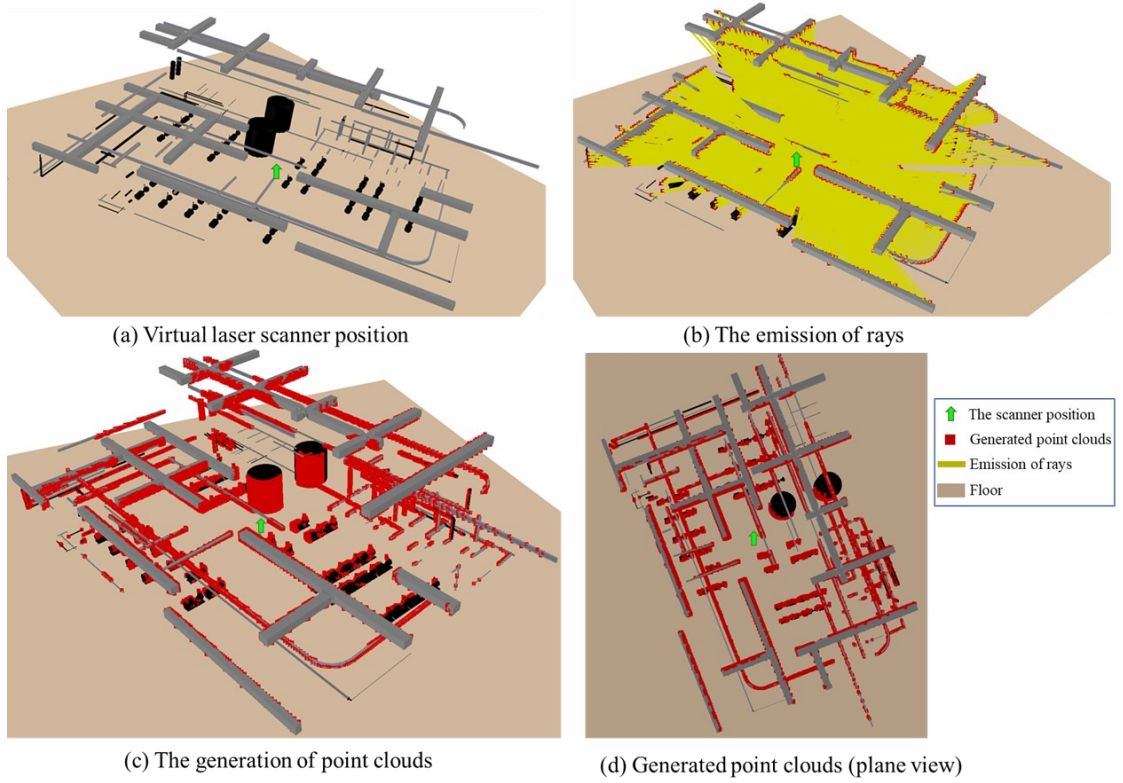


Figure 2: Synthetic point cloud generation process using the proposed RBLsIA method.

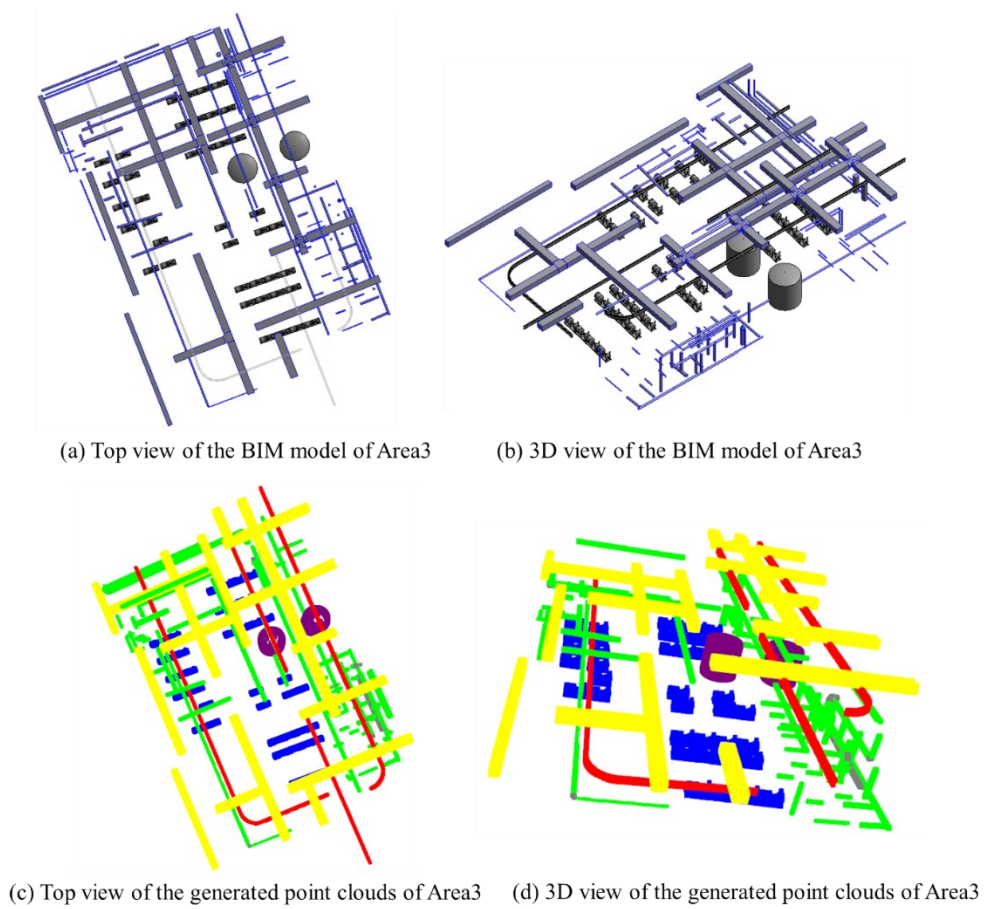


Figure 3: The BIM model and generated point clouds of Area3.

Data Preparation

The PSNET5 dataset (Yin et al., 2023) is used in this study to validate the proposed approach. The initial scene includes 500 million raw data points, covering approximately 3700 square meters, and consists of four areas with different scenes, as shown in Table 1.

Table 1: The number of points of each semantic category of the PSNET5 dataset.

| Area | Scene | ibeam | pipe | pump | rbeam | tank | Total |
|-------|-------|-----------|------------|-----------|------------|-----------|------------|
| Area1 | CH | 359,610 | 22,799,721 | 1,478,449 | 5,821,433 | 0 | 30,459,213 |
| Area2 | OSCG | 467,782 | 5,712,622 | 5,712,622 | 2,488,327 | 5,455,825 | 14,404,173 |
| Area3 | SPH | 3,023,003 | 8,408,907 | 2,455,212 | 9,055,639 | 1,523,331 | 24,466,092 |
| Area4 | WRT2 | 656,071 | 3,052,706 | 836,554 | 7,040,629 | 0 | 11,585,960 |
| Total | | 4,506,466 | 39,973,956 | 5,049,832 | 24,406,028 | 6,979,156 | 80,915,438 |

Experimental Settings

This study employed ResPointNet++ as the DL algorithm (Yin et al., 2023). Each experiment was conducted over 100 epochs, utilizing the SGD optimizer with an initial learning rate of 0.01 and cross-entropy as the loss function. All experiments were performed on a single NVIDIA GTX 4090 GPU, with each set taking approximately 12 hours to complete. Due to the inconsistent color standards and varying reflections in MEP components, the input channels were limited to XYZ coordinates, excluding color information.

To evaluate the performance of DL models, three metrics were used: Overall Accuracy (OA), Intersection over Union (IoU), and mean IoU (mIoU). OA provides an overall measure of accuracy by indicating the proportion of correctly predicted points relative to the total. IoU assesses segmentation quality for each class by measuring the overlap between predicted and actual segments. In contrast, mIoU offers a balanced evaluation across all N classes, highlighting the model's consistent performance across different object types. The formulas for these metrics are presented in Equations (1), (2), and (3).

$$OA = \frac{\text{Number of correctly classified points}}{\text{Total number of points}} \quad (1)$$

$$IoU = \frac{\text{True Positive}}{\text{True Positive} + \text{False Positive} + \text{False Negative}} \quad (2)$$

$$mIoU = \frac{1}{N} \sum_{i=1}^n IoU_i \quad (3)$$

Experiment Design

The validation experiments consist of three parts. First, the performance of the uniform sampling method and the RBLISIA sampling method for generating synthetic point clouds was compared. Second, the performance of semantic segmentation was evaluated by comparing models trained on real point clouds with those trained on synthetic point clouds. Third, the impact of increasing the number of synthetic point cloud samples on semantic

segmentation results was analyzed. Finally, the effectiveness of synthetic point clouds was assessed in a different scene.

segmentation results was analyzed. Finally, the effectiveness of synthetic point clouds was assessed in a different scene.

Results

Comparison of Different Generation Methods for Synthetic Point Clouds

This section aimed to compare the performance of two different generation methods for synthetic point clouds: uniform sampling method and RBLISIA sampling method. As shown in Table 2, five CGs (A to E) were conducted with different training sets and test sets, where some used purely synthetic data for training while some others used a mix of real and synthetic data for training.

According to the comparison results, it is clear that using synthetic point clouds generated by the RBLISIA method could always yield better model performance than using data from the uniform sampling method. On average, the RBLISIA method could achieve an improvement of 2.13% and 3.32% in OA and mIoU, respectively. Among all IoU metrics, the tank category showed the most significant improvement of 38.38%, followed by pump of 5.47%, rbeam of 2.41%, pipe of 1.55%, and ibeam of -1.76%. The substantial improvements in the tank and pump categories may be attributed to these being minority classes. For minority classes, more realistic synthetic point cloud features help in learning more accurate characteristics, thereby improving the precision of these categories. The average performance of the RBLISIA method on ibeam was slightly worse than that of uniform sampling. This is possibly because ibeam is relatively slender, making it difficult for the RBLISIA method to include its complete features, whereas uniform sampling is more likely to include complete features. Overall, the results demonstrate that the RBLISIA sampling method provides better model performance compared to uniform sampling method. Thus, the RBLISIA sampling method was adopted in the following experiments.

Table 2: Comparison between uniform sampled synthetic point clouds and RBLISIA sampled synthetic point clouds

| CG | Exp. No. | Training set | Test set | OA (%) | mIoU (%) | IoU (%) | | | | |
|----|----------|-------------------------------------|----------|--------------|--------------|---------|-------|-------|-------|-------|
| | | | | | | ibeam | pipe | pump | rbeam | tank |
| A | 1 | Area2 RBLISIA synthetic | Area3 | 64.62 | 45.46 | 56.45 | 48.74 | 0.02 | 69.23 | 64.62 |
| | 2 | Area2 uniform synthetic | Area3 | 63.19 | 42.85 | 66.73 | 54.08 | 0 | 67.18 | 26.24 |
| B | 3 | Area3 RBLISIA synthetic | Area4 | 85.52 | 68.05 | 98.30 | 50.58 | 26.14 | 97.19 | / |
| | 4 | Area3 uniform synthetic | Area4 | 83.64 | 63.56 | 97.76 | 45.53 | 21.32 | 89.64 | / |
| C | 5 | Area1 RBLISIA synthetic, Area3 real | Area4 | 95.22 | 89.10 | 95.97 | 85.22 | 78.76 | 96.46 | / |
| | 6 | Area1 uniform synthetic, Area3 real | Area4 | 93.28 | 83.09 | 97.05 | 75.26 | 63.92 | 96.15 | / |
| D | 7 | Area1+Area3 RBLISIA synthetic | Area4 | 96.30 | 90.06 | 95.23 | 84.89 | 81.41 | 94.79 | / |
| | 8 | Area1+Area3 uniform synthetic | Area4 | 93.76 | 89.64 | 93.23 | 88.65 | 79.91 | 96.78 | / |
| E | 9 | Area2+Area3 RBLISIA synthetic | Area1 | 81.69 | 74.38 | 68.67 | 87.04 | 74.03 | 67.79 | / |
| | 10 | Area2+Area3 uniform synthetic | Area1 | 78.81 | 71.33 | 68.63 | 85.18 | 67.83 | 63.67 | / |

Comparison of Training with Real and Synthetic Point Clouds with Different Data Sizes

Table 3 shows that, given the same training data size, training with synthetic point clouds results in worse performance compared to real point clouds. However, a key advantage of synthetic point clouds is the lower cost of generating labeled datasets. This section investigates whether increasing the training data size can enhance model performance when using synthetic point clouds.

As shown in Table 4, totally five CGs (F to J) were implemented. In each CG, the training set contained only one area when training with real point clouds, while the training set contained one or two areas when training with synthetic point clouds. In all the five CGs, it is found that training with synthetic point clouds of two areas could generate better performance than training with synthetic point clouds of only one area, with an average improvement of 13.91% for OA and 24.58% for mIoU. Hence, it is concluded that increasing the training data size could effectively improve the model performance when training with synthetic point clouds.

Among all the five CGs, three of them (CG-F, CG-G, and CG-H) showed that training with synthetic point clouds of two areas could yield better performance than training with real point clouds of only one area. This indicated that, with a larger training data size, purely using synthetic point clouds was able to achieve better performance than using real point clouds.

Effects in the different MEP scenario

To further evaluate the generalization capability of the point cloud generation method in various environments, this study scanned a new underground garage scene at Southeast University. This scene includes both building components, such as ceilings, floors, pillars, walls, and doors, as well as MEP components, such as air ducts, fire hydrants, and pipes. The scanned scene was divided into

Scene2-Area1, Scene2-Area2, and Scene2-Area3. The scanned scene for Scene2-Area1 is illustrated in Figure.4(a). Subsequently, a BIM model was manually created based on Scene2-Area2, as shown in Figure.4(b). Synthetic point clouds of Scene2-Area2 were generated using the RBLISIA method, with the simulated laser scanning station locations depicted in Figure.4(c), and the final generated point cloud scene presented in Figure.4(d). In this experiment, CG-K compared the performance of two different generation methods for synthetic point clouds. While CG-L explored the effects of supplementing real point clouds with synthetic point clouds for model training. As shown in Table 4, the RBLISIA method in CG-K achieved higher OA and mIoU compared to the uniform method. Notably, the mIoU for the air duct, ceiling, fire hydrant, and door categories in the uniform method was 0, indicating that uniform synthetic point clouds may not be suitable for this scene. In contrast, the RBLISIA synthetic method demonstrated better results across all categories. Additionally, CG-L demonstrated that supplementing real samples with synthetic point clouds further improved both mIoU and OA. This indicates that the use of the RBLISIA method can effectively enhance semantic segmentation accuracy in the underground garage scene

Table 3: Comparison between uniform sampled synthetic point clouds and RBLsIA sampled synthetic point clouds

| CG | Exp. No. | Training set | Test set | OA(%) | mIoU (%) | IoU (%) | | | | |
|----|----------|-----------------------|----------|--------------|--------------|---------|-------|-------|-------|-------|
| | | | | | | ibeam | pipe | pump | rbeam | tank |
| F | 11 | Area1 real | Area4 | 91.55 | 69.30 | 39.13 | 79.56 | 66.4 | 92.11 | / |
| | 12 | Area1 synthetic | Area4 | 82.49 | 56.15 | 39.29 | 47.73 | 50.25 | 87.34 | / |
| | 7 | Area1+Area3 synthetic | Area4 | 96.30 | 90.06 | 95.23 | 84.89 | 81.41 | 94.79 | / |
| G | 13 | Area3 real | Area4 | 92.85 | 80.31 | 97.06 | 73.23 | 53.89 | 97.05 | / |
| | 14 | Area3 synthetic | Area4 | 85.52 | 68.05 | 98.30 | 50.58 | 26.13 | 97.19 | / |
| | 7 | Area1+Area3 synthetic | Area4 | 96.30 | 90.06 | 95.23 | 84.89 | 81.41 | 94.79 | / |
| H | 15 | Area2 real | Area4 | 71.57 | 35.37 | 42.63 | 23.01 | 0 | 75.64 | / |
| | 1 | Area2 synthetic | Area4 | 51.48 | 29.17 | 45.78 | 28.02 | 0.00 | 42.89 | / |
| | 9 | Area2+Area3 synthetic | Area4 | 89.52 | 70.84 | 97.11 | 56.83 | 30.94 | 98.47 | / |
| I | 11 | Area1 real | Area3 | 77.00 | 64.82 | 73.85 | 56.59 | 49.75 | 79.08 | / |
| | 12 | Area1 synthetic | Area3 | 70.99 | 56.11 | 56.58 | 41.89 | 50.09 | 75.87 | / |
| | 16 | Area1+Area2 synthetic | Area3 | 73.42 | 56.77 | 46.75 | 55.13 | 53.13 | 72.09 | 56.77 |
| J | 13 | Area3 real | Area1 | 90.70 | 90.98 | 79.76 | 96.87 | 97.54 | 89.77 | / |
| | 14 | Area3 synthetic | Area1 | 77.21 | 49.74 | 45.58 | 74.11 | 28.12 | 51.15 | / |
| | 9 | Area2+Area3 synthetic | Area1 | 81.69 | 74.38 | 68.67 | 87.04 | 74.03 | 67.79 | / |

Table 4: Effects of RBLsIA method in the underground garage scene.

| CG | Exp. No. | Training set | Test set | OA(%) | mIoU (%) | IoU (%) | | | | | | | |
|----|----------|--|--------------|-------|----------|----------|---------|--------------|-------|--------|-------|-------|-------|
| | | | | | | air duct | ceiling | fire hydrant | floor | pillar | pipe | wall | door |
| K | 17 | Scene2-Area1 uniform synthetic | Scene2-Area2 | 44.56 | 23.18 | 0.00 | 0.00 | 0.00 | 55.57 | 42.30 | 16.26 | 71.27 | 0 |
| | 18 | Scene2-Area1 RBLsIA synthetic | Scene2-Area2 | 82.10 | 59.37 | 44.63 | 90.57 | 58.79 | 97.43 | 44.94 | 45.35 | 62.32 | 30.93 |
| L | 19 | Scene2-Area3 | Scene2-Area2 | 89.98 | 72.39 | 1.75 | 96.46 | 65.18 | 99.79 | 52.38 | 89.24 | 82.83 | 91.50 |
| | 20 | Scene2-Area1 RBLsIA synthetic + Scene2-Area3 | Scene2-Area2 | 90.29 | 75.32 | 40.69 | 95.00 | 55.08 | 99.76 | 55.14 | 88.99 | 80.99 | 86.90 |

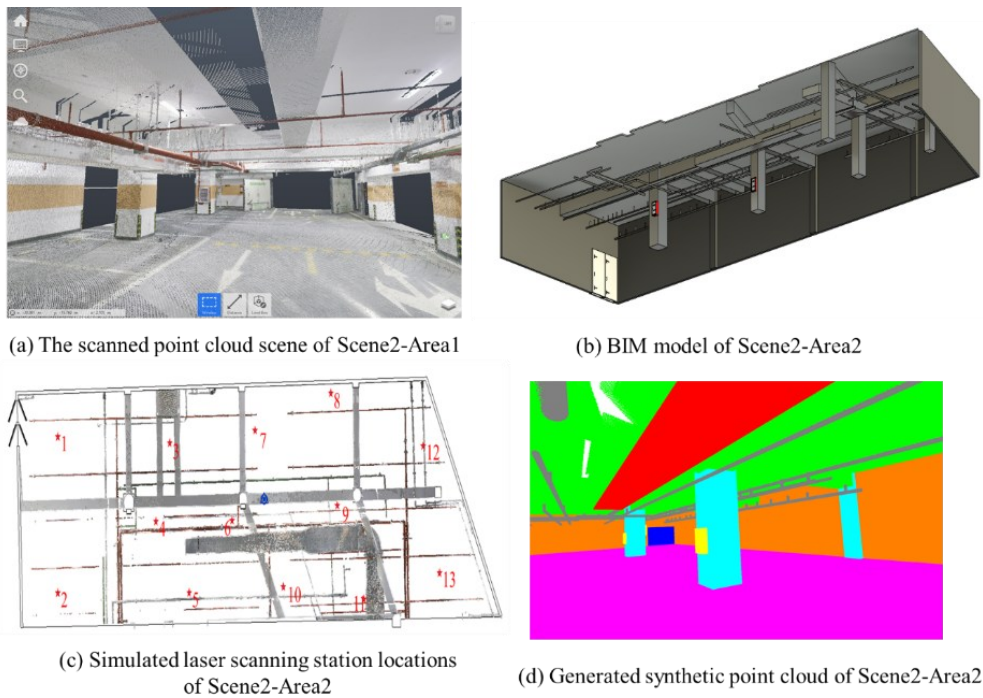


Figure 4: Scanned point cloud scene and generated BIM models or point clouds of Scene2-Area. (a) Scanned point cloud scene of Scene2-Area1, (b) BIM model of Scene2-Area2, (c) Simulated laser scanning station locations of Scene2-Area2, (d) Generated synthetic point cloud of Scene2-Area2

Conclusions

This study proposed the RBLSIA to automatically generate synthetic point clouds for MEP from BIM models. A total of 20 comparative experiments were carried out to evaluate the semantic segmentation performance across different methods for synthetic point cloud generation, and different training datasets. The experimental results indicated that: 1) the mIoU with synthetic point clouds produced by the RBLSIA method is on average 3.32% higher than that by the uniform sampling method; 2) increasing the number of synthetic point cloud samples further improved both the OA and mIoU for semantic segmentation, even surpassing the training accuracy achieved with real point clouds.

The results also reveal a gap between synthetic and real point clouds, particularly for components with significant differences between BIM models and real objects (such as pumps). Future research should focus on reducing these discrepancies to further enhance the quality of synthetic point clouds. Additionally, future studies could explore the impact of neuroengineering on field-collected point cloud data from the perspectives of neuroengineering and qualitative simulation, and investigate the relationship between point cloud data and model reconstruction (Yue et al., 2024b; Yue et al., 2024c).

Acknowledgments

This work was supported by the National Key R&D Program of China (No. 2023YFC3804300), Start-up Research Fund of Southeast University (No.

RF1028623126) and Jiangsu Provincial Science and Technology Program (Hong Kong, Macao, and Taiwan Science and Technology Cooperation Project), Grant No. BZ2024058, SEU Innovation Capability Enhancement Plan for Doctoral Students (No. CXJH_SEU 25101).

References

- Lamas, D., Justo, A., Soilán, M., Riveiro, B., 2024. Automated production of synthetic point clouds of truss bridges for semantic and instance segmentation using deep learning models. *Automation in Construction* 158, 105176.
- Tang, S., Li, X., Zheng, X., Wu, B., Wang, W., Zhang, Y., 2022. BIM generation from 3D point clouds by combining 3D deep learning and improved morphological approach. *Automation in Construction* 141, 104422.
- Tang, S.J., Huang, H.S., Zhang, Y.J., Yao, M.M., Li, X.M., Xie, L.F., Wang, W.X., 2023. Skeleton-guided generation of synthetic noisy point clouds from as-built BIM to improve indoor scene understanding. *Automation in Construction* 156, 105076.
- Wang, Q., Li, J.J., Tang, X.Y., Zhang, X.C., 2022. How data quality affects model quality in scan-to-BIM: A case study of MEP scenes. *Automation in Construction* 144, 104598.
- Wang, Q., Tan, Y., Mei, Z.Y., 2020. Computational Methods of Acquisition and Processing of 3D Point

- Cloud Data for Construction Applications. *Archives of Computational Methods in Engineering* 27, 479-499.
- Won, J., Czerniawski, T., Leite, F., 2020. Semantic segmentation of point clouds of building interiors with deep learning: Augmenting training datasets with synthetic BIM-based point clouds. *Automation in Construction* 113, 103144.
- Xiong, X.H., Adan, A., Akinci, B., Huber, D., 2013. Automatic creation of semantically rich 3D building models from laser scanner data. *Automation in Construction* 31, 325-337.
- Yin, C., Wang, B., Gan, V.J., Wang, M., Cheng, J.C., 2021. Automated semantic segmentation of industrial point clouds using ResPointNet++. *Automation in Construction* 130, 103874.
- Yin, C., Yang, B., Cheng, J.C.P., Gan, V.J.L., Wang, B.Y., Yang, J., 2023. Label-efficient semantic segmentation of large-scale industrial point clouds using weakly supervised learning. *Automation in Construction* 148.
- Yue, H., Wang, Q., Yan, Y., Huang, G., 2025. Deep learning-based point cloud completion for MEP components. *Automation in Construction* 175, 106218.
- Yue, H., Wang, Q., Zhao, H., Zeng, N., Tan, Y., 2024a. Deep learning applications for point clouds in the construction industry. *Automation in Construction* 168, 105769.
- Yue, H.Z., Ye, G., Cao, H.Y., Liu, Q.J., Xiang, Q.T., Luo, Y.L., 2024b. Exploring the Internal Influence Mechanism of Group Safety Behavior of Construction Workers: Qualitative Method Approach. *Journal of Construction Engineering and Management* 150.
- Yue, H.Z., Ye, G., Liu, Q.J., Yang, X.H., Xiang, Q.T., Luo, Y.L., 2024c. Impact of Cognitive Fatigue on Attention and the Implications for Construction Safety: A Neuroscientific Perspective. *Journal of Construction Engineering and Management* 150.
- Zhai, R.M., Zou, J.G., He, Y.F., Meng, L.Y., 2022. BIM-driven data augmentation method for semantic segmentation in superpoint-based deep learning network. *Automation in Construction* 140, 104373.
- Zhang, H.X., Zou, Z.B., 2023. Quality assurance for building components through point cloud segmentation leveraging synthetic data. *Automation in Construction* 155, 105045.
- Zhang, Z., Ji, A., Wang, K., Zhang, L., 2022. UnrollingNet: An attention-based deep learning approach for the segmentation of large-scale point clouds of tunnels. *Automation in Construction* 142, 104456.